XXII. Washburn Extraction Routine and Width of the Point Spread Function in Low Dispersion non-GEOM IUE Images

Klaas S. de Boer * and Marilyn R. Meade
Washburn Observatory and Space Astronomy Laboratory
University of Wisconsin, Madison, WI 53706

* Now at Astronomisches Institut, Universität Tübingen
7400 Tübingen 1, Federal Republic of Germany

The new low dispersion extraction methods in use at the IUE Observatory since November 1980 show that the Point Spread Function (PSF) in these spectra is narrower than the PSF found in images processed with the older reduction methods.

The new software to reduce IUE images, implemented at the IUE Observatory on November 3, 1980, differs in two important aspects from the earlier IUESIPS package. First, the images are not geometrically rectified, a procedure which was based on the location of the fiducial marks in the images. (This implies that the wavelength calibration of the spectra may be nonlinear, this calibration now being implicitly based on the location of the fiducial marks.) The photometric correction, therefore, is applied directly to the raw image. Secondly, the wavelength step of the spectral resolution is made smaller (doubled from earlier methods) and is now equivalent to 1.2 Å in SWP and 1.9 Å in LWR. For a discussion of this new method, see Bohlin, Lindler and Turnrose (1981). Since the Washburn Extraction Routine has always used the wavelength steps of 1.2 Å and 1.9 Å in SWP and LWR respectively, our interest in the new IUE Observatory software is in its non-geom aspect (for a comparison of extraction methods, see de Boer and Snijders 1981).

Upon our request, the IUE Observatory has re-reduced 8 old images with the new non-geom method, 4 images each of SWP and LWR. All but one SWP image contains both large and small aperture spectra. We have extracted these images with the Washburn Extraction Routine [Koornneef and de Boer (1979) and de Boer, Koornneef and Meade (1980)] in the mode to determine the width σ of the point spread function. The 8 images selected were known to have gaussian PSF's throughout their spectra (see de Boer, Koornneef and

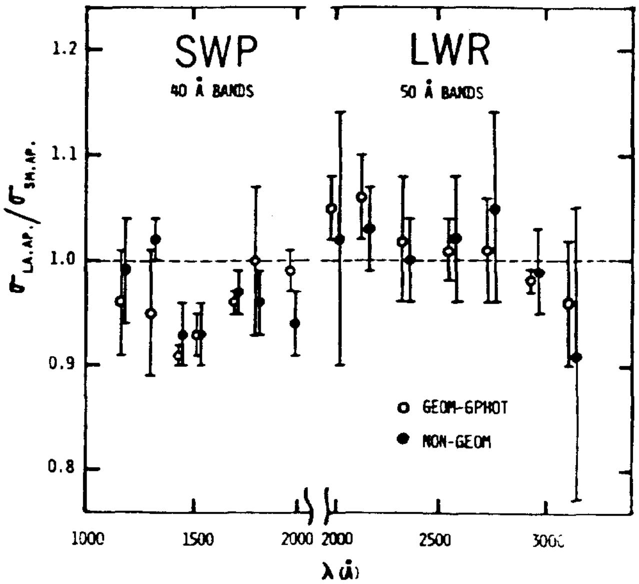

Fig. 1: Ratio $\sigma_{la.ap.}/\sigma_{sm.ap.}$ for a gaussian Point Spread Function of IUE low dispersion spectra processed by the geom-gphot and the new non-geom reduction methods versus wavelength. Average of 3 images in SWP and 4 images in LWR, with standard deviations given.

and Meade 1980):

$$I(x) = B + \frac{I}{\sqrt{2\pi\sigma^2}} \exp\left[-\frac{1}{2}\left(\frac{x-x_0}{\sigma}\right)^2\right]$$

where I and B are the spectral and background intensities respectively, σ is the width of the point spread function, x_0 the central position of the spectrum, and x is the position of the other pixels on a particular diagonal (almost) perpendicular to the dispersion. Here x and σ are given in units of length equal to $\sqrt{2} \times$ pixel length, where a pixel is the image sample spacing.

The results are shown in the figures. Average σ's were determined in 40 Å and 50 Å wide segments of the spectra for SWP and LWR respectively, in both the large and the small apertures. The results for the two apertures are essentially identical (see Fig. 1). Figure 2 shows the grand mean σ's of the 4 images in each camera in the respective wavelength bands. The σ's of the non-geom SWP images are 8 ± 3% less than the σ's of the same images processed with the earlier geom-gphot method. In LWR the effect is about the same, 7 ± 3%. The PSF appears to be narrowest at wavelengths which are nearest to the center of the cameras.

The actual σ in the non-geom image is smaller than in the geom-gphot image as processed earlier. This implies that the elimination of the geom correction results in

a) avoidance of photometric distortion from the curved ITF due to

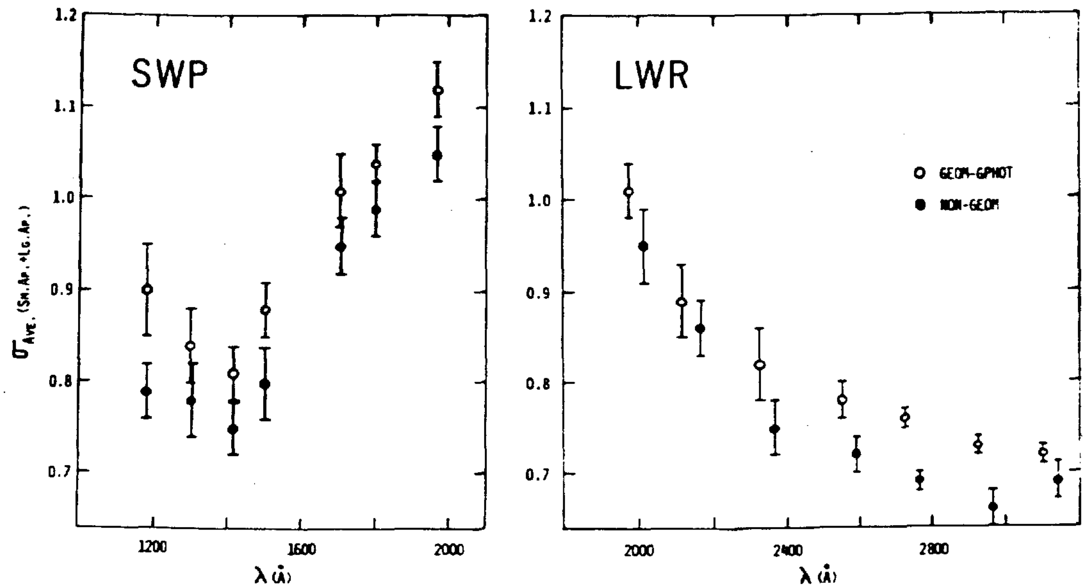

Fig. 2: Wavelength dependence of the width σ of a gaussian PSF of IUE low dispersion images processed by both the geom-gphot and the non-geom methods. Average of 4 images in each camera, with standard deviations also given.

resampling in the raw images (for examples of ITF's, see Bohlin et al. (1980))

b) a better separation of echelle orders in high dispersion images

c) retaining the intrinsic spectral resolution

Figure 3 shows the curvatures of the SWP and LWR spectra for both the geom-gphot and non-geom methods in both apertures. We can see that the curvature in the SWP spectrum in the non-geom method is essentially the same as in the earlier geom-gphot method. The LWR spectrum is strongly curved in the new method, like it is in the raw image (as we know from histograms on the Experimental Display System on the IUE Observatory).

References

Bohlin, R.C., Holm, A.V., Savage, B.D., Snijders, M.A.J., and Sparks, W.M. 1980, Astron. and Astrop., 85, 1.

Bohlin, R.C., Lindler, D.J. and Turnrose, B.E. 1981, IUE NASA Newsletter No. 12, page 9.

de Boer, K.S., Koornneef, J., and Meade, M.R. 1980, in The Universe at Ultraviolet Wavelengths: The First Two Years of IUE, Ed. R.D. Chapman, NASA CP 2171, p 771 .

de Boer, K.S. and Snijders, M.A.J. 1981, Proceedings IUE Data Reduction Workshop, Vienna, and IUE NASA Newsletter, XIV p 154 .

Koornneef, J. and de Boer, K.S. 1979, IUE NASA Newsletter No. 5; and IUE SRC Newsletter No. 4, p. 41.

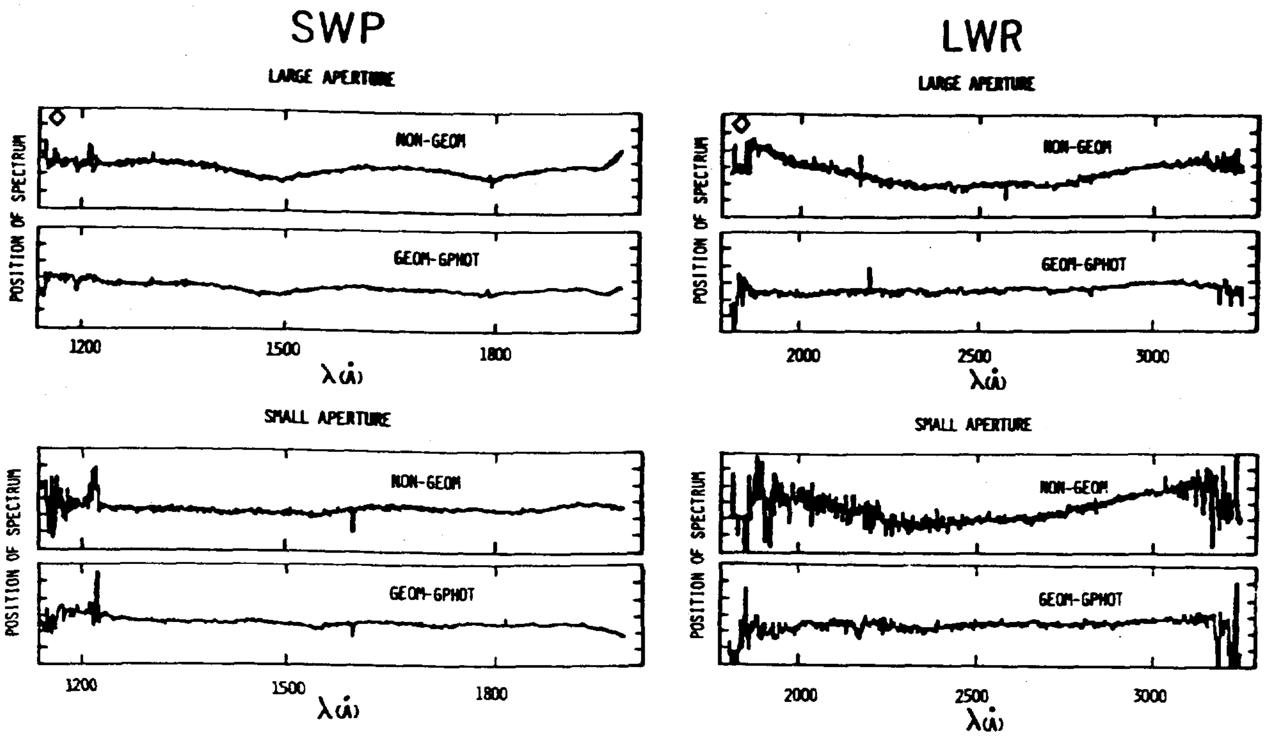

Fig. 3: Comparison of the position of IUE low dispersion spectra as processed by the non-geom and geom-gphot reduction schemes as a function of wavelength for both the large and small apertures. The position is given in units of $\sqrt{2}$ pixel per division on the ordinate. A lower value of the position is toward the center of the camera.